Optimal Charging in Wireless Rechargeable Sensor Networks

Lingkun Fu, *Student Member, IEEE*, Peng Cheng, *Member, IEEE*, Yu Gu, *Member, IEEE*, Jiming Chen, *Senior Member, IEEE*, and Tian He, *Senior Member, IEEE*

***Abstract*—Recent years have witnessed several new promising technologies to power wireless sensor networks, which motivate some key topics to be revisited. By integrating sensing and computation capabilities to the traditional radio-frequency identification (RFID) tags, the Wireless Identification and Sensing Platform (WISP) is an open-source platform acting as a pioneering experimental platform of wireless rechargeable sensor networks. Different from traditional tags, an RFID-based wireless rechargeable sensor node needs to charge its onboard energy storage above a threshold to power its sensing, computation, and communication components. Consequently, such charging delay imposes a unique design challenge for deploying wireless rechargeable sensor networks. In this paper, we tackle this problem by planning the optimal movement strategy of the mobile RFID reader, such that the time to charge all nodes in the network above their energy threshold is minimized. We first propose an optimal solution using the linear programming (LP) method. To further reduce the computational complexity, we then introduce a heuristic solution with a provable approximation ratio of $(1+\theta)/(1-\varepsilon)$ by discretizing the charging power on a 2-D space. Through extensive evaluations, we demonstrate that our design outperforms the set-cover-based design by an average of 24.7%, whereas the computational complexity is $\mathcal{O}((N/\varepsilon)^2)$. Finally, we consider two practical issues in system implementation and provide guidelines for parameter setting.**

***Index Terms*—Charging delay, energy efficient, energy harvesting, mobile charging, sensor networks, wireless charging.**

I. Introduction

ONE fundamental issue in the Wireless Identification and Sensing Platform (WISP) is the energy provisioning problem, i.e., how to distribute energy in an optimal manner to power a network [2]–[18]. As most existing sensor networks are powered by batteries, their lifetime is limited by the storage capacity of the battery used. The recent breakthrough in wireless energy transfer technology developed by Kurs *et al.* [19] has provided a promising alternative to power these sensor nodes. We expect that, in the near future, a new class of wireless rechargeable sensor networks will have potential to bring universal sensing, communication, and computation capabilities to our daily life. For example, without batteries attached to a node, we can design much smaller and more flexible sensor nodes that can be attached to objects such as fruit and medical pills, which are not traditionally instrumented. Clearly, by providing real-time monitoring capabilities to our critical daily products, we have the potential to significantly improve the quality of living for the general public.

Many pioneering works have focused on the internal microelectronic design [20]–[22] to improve the energy charging efficiency for wireless rechargeable sensor networks. While it is essential to improve the fundamental microelectronics design for wireless energy transfer systems, we observe that, in the practical applications, the charging time of individual wireless rechargeable sensor node is either not negligible and should play an important role in overall system performance. For a typical wireless rechargeable sensor node, such as Intel Research's WISP [23], a sensor node has to be wirelessly charged above a certain energy threshold in order for various sensing, computation, and communication components to function properly. For example, through our empirical measurement, we observe that the charging time for voltage to reach 1.8 V to power a WISP equipped with a 100-μF capacitor can be as large as 155 s, when the radio-frequency identification (RFID) reader is 10 m away.

Another consideration for a practical wireless rechargeable sensor network is that RFID readers are normally much more expensive than wireless rechargeable sensor nodes (about 100 times price difference [24]). Hence, we would normally need one or more readers that are carried by robots [25]–[28] or move along an existing infrastructure, such as moving tracks, to efficiently power all nodes in the network [24]. Therefore, it is essential to plan the movement pattern of RFID readers to minimize the total charging delay of the network.

In this paper, we consider the scenario that an RFID reader moves and stops at several locations to wirelessly charge nodes and obtain readings of interests at its surroundings. Such a scenario can be found in various types of industry settings, e.g., in warehouse inventory management [29] or in large distribution center [24]. Our optimization objective, therefore, is to identify

Manuscript received April 13, 2014; revised November 24, 2014; accepted December 27, 2014. Date of publication January 12, 2015; date of current version January 13, 2016. This work was supported in part by the National Natural Science Foundation of China under Grant 61228302, by ZJSF under Grant LY14F030016, and by the National Program for Special Support of Top Notch Young Professionals, Fundamental Research Funds for the Central Universities, 2014XZZX001-03. Part of this paper was presented at IEEE Infocom 2013, Turin, Italy [1]. The review of this paper was coordinated by Prof. J. Misic. *(Corresponding author: Peng Cheng.)*

L. Fu, P. Cheng, and J. Chen are with the State Key Laboratory of Industrial Control Technology, Zhejiang University, Hangzhou 310027, China (e-mail: lkfu@iipc.zju.edu.cn; pcheng@iipc.zju.edu.cn; jmchen@iipc.zju.edu.cn).

Y. Gu is with IBM Research-Austin, Austin, TX 78758 USA (e-mail: yugu@us.ibm.com).

T. He is with the School of Electronic Information and Electronic Engineering, Shanghai Jiaotong University, Shanghai 200240, China, and also with the Department of Computer Science and Engineering, University of Minnesota, Minneapolis, MN 55455 USA (e-mail: tianhe@cs.umn.edu).

Color versions of one or more of the figures in this paper are available online at http://ieeexplore.ieee.org.

Digital Object Identifier 10.1109/TVT.2015.2391119

the optimal reader stop locations and the corresponding stop duration such that the total delay to charge all nodes in the network above their energy threshold is minimized. The major contributions of this paper are as follows.

- We identify charging delay as one of the key design hurdles in wireless rechargeable sensor networks and introduce an effective solution to minimize charging delay in such networks. To the best of our knowledge, this is the first work that provides a general framework to minimize charging delay in wireless rechargeable sensor networks.
- We formulate the charging delay minimization problem as a linear programming (LP) problem, which can be optimally solved to identify the optimal reader stop locations and the corresponding stop duration.
- We use the concepts of the smallest enclosing space (SES) and further a space discretization method [30] to significantly reduce the searching area for the optimal solution with an $1/(1-\varepsilon)$ approximation ratio. The optimal solution may consist a large number of stop locations; for practical consideration, we further introduce a location merging scheme to reduce the number of stop locations while maintaining the charging delay to an $(1+\theta)$ upper bound.
- We further investigate our design performance with a practical issue that the sensor nodes are deployed with location uncertainty. Then, we address another practical issue by using a heuristic method to optimally sequence the reader stop order to obtain a smoother network charging performance by avoiding a sharp increase in the number of fully charged nodes.

The remainder of this paper is organized as follows. Section II describes our energy rechargeable platform and its charging model. In Section III, we introduce our problem formulation and present a heuristic solution to the problem. Section IV investigates two practical issues after obtaining the optimal solution. We evaluate our design in Section V. Section VI discusses related works, and we conclude this paper in Section VII.

II. Preliminaries

A. Wireless Identification and Sensing Platform

WISP, which has been developed by Intel Research [23], is one of the most representative platform of wireless rechargeable sensor nodes. A WISP node not only inherits the capabilities of traditional RFID tags but also supports sensing and computing. When close to an RFID reader, the WISP node can harvest energy from the signals emitted by the reader. The charged energy is stored in a capacitor and can be used for future data sensing, logging, computing, and transferring [31].

B. Energy Charging Model

In this paper, we use the WISP reader charging model proposed in [2] as follows:

$$P_r = \frac{G_s G_r \eta}{L_p}\left(\frac{\lambda}{4\pi(d+\beta)}\right)^2 P_0 \tag{1}$$

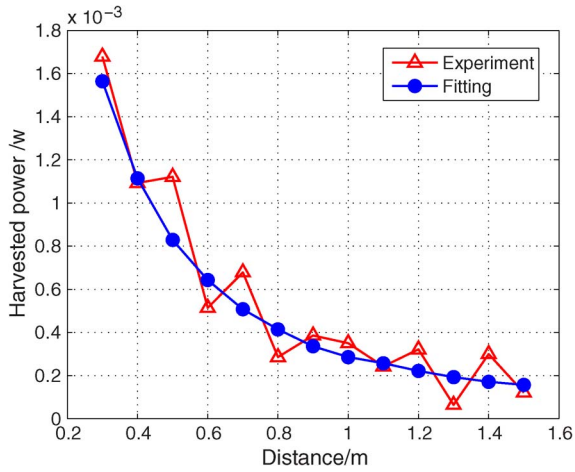

Fig. 1. Experiment and energy charging model for the harvested power under different distances.

where d is the distance between the sensor node and the RFID reader, P_0 is the source power, G_s is the source antenna gain, G_r is the receive antenna gain, L_p is the polarization loss, λ is the wavelength, η is the rectifier efficiency, and β is a parameter to adjust the *Friis*' free space equation for short distance transmission. Except for distance d, all other parameters in (1) are constant values based on the environment and device settings. This model is based on the *Friis*' free space equation and has been experimentally shown to be a good approximation of charged energy in [2]. To further validate this charging model, we perform additional experiments to investigate the charged power by varying distances between the reader and the sensor node. As shown in Fig. 1, the measured harvested power matches (1) well during our experiments.

To ease the description of design in the following, we simplify the charging model in (1) as

$$P_r = \frac{\alpha}{(d+\beta)^2} \tag{2}$$

where d is the distance from a sensor node to the reader, and α represents other constant environment parameters, including P_0, G_s, G_r, L_p, λ, and η in (1).

Here, we would emphasize that our design does not depend on any specific charging model. As long as the charging power shows a trend of negative correlation with the charging distance, which is true in most practical settings [19], this paper can be directly applied under these models.

III. Main Design

A. Problem Formulation

We assume a network deployment with N stationary wireless rechargeable sensor nodes. Every node i in the network can be localized using techniques in [32]–[35] and represented as (W_x^i, W_y^i). We also assume that there is an RFID reader that is able to move around with a robot [25]–[27] or along an existing infrastructure (moving tracks, etc.) [24]. When nodes are close to an RFID reader, they charge their internal energy storage and are able to perform functionalities such as sensing,

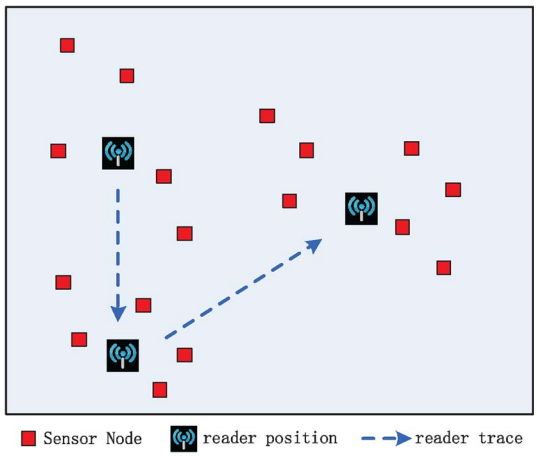

Fig. 2. Wireless rechargeable sensor network and reader stop positions.

computation, and communication when the charged energy is above a threshold δ. Therefore, to minimize the total duration for all nodes in the network to complete their temporal tasks, we need to find out the optimal strategy to minimize the charging delay for all nodes in the network. Specifically, in this paper, we are aiming at finding the optimal stop locations and the corresponding stop duration of the RFID reader to minimize the charging delay in the network. Fig. 2 shows an example of a reader stopping at three locations to charge nodes in the network.

To formulate this charging problem, let us first assume that the reader stops at several different locations and denote the location of its jth stop as (R_x^j, R_y^j) and the corresponding stop duration as t_j. Consequently, the distance between the jth reader stop location and node i is $d_{ij} = \sqrt{(W_x^i - R_x^j)^2 + (W_y^i - R_y^j)^2}$, and the corresponding charging power is $P_{ij} = \alpha/(d_{ij} + \beta)^2$ based on (2). The accumulated energy of node i at the jth reader stop location is $P_{ij}t_j$. Given an area of interest with N sensor nodes, the node charged energy threshold δ and the RFID reader can stop at any location in this continuous space; we can mathematically formulate the optimization problem of minimizing charging delay of all nodes in the network as

$$\min \quad T = \sum_{j=1}^{\infty} t_j \tag{3}$$

$$\text{s.t.} \quad \sum_{j=1}^{\infty} P_{ij} t_j \geq \delta, \quad (i \in N) \tag{4}$$

where

$$P_{ij} = \frac{\alpha}{(d_{ij} + \beta)^2}, \quad (i \in N, j \in (1, 2, \ldots, \infty)) \tag{5}$$

$$d_{ij} = \sqrt{\left(W_x^i - R_x^j\right)^2 + \left(W_y^i - R_y^j\right)^2}. \tag{6}$$

For a static wireless rechargeable sensor network with N nodes, when the stop locations of the reader are given *a priori*, then the distances between the reader and each node i in the network are also fixed [as shown in (6)]. Consequently, the charging power from the reader's jth location to a node i, which we term as P_{ij}, can also be determined by (5). To find the minimal charging duration for the whole network and solve (3), we can simply use the existing LP methods [36] to obtain the optimal stop duration at each of these stops for the RFID reader.

If the stop locations of the reader are not given *a priori*, to find the optimal reader stop locations and the corresponding stop duration for (3), the most straightforward method is to include all possible stop locations of the RFID reader in the LP solver. However, this simple method incurs very high computational overhead and is not suitable for most practical applications. Therefore, in the following, we introduce a set of new techniques to reduce effectively the dimension of search space of reader stop locations while still maintaining provable system performance.

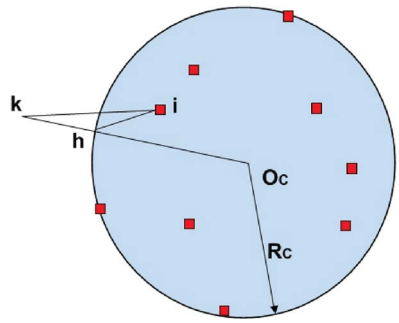

Fig. 3. Reader must stop within the SES disk.

B. Smallest Enclosing Space

Inspired by Welzl's work on the smallest enclosing disk [37], we observe that the search space of reader stop locations can be reduced to the *SES*, which is the smallest circular disk that covers all N wireless rechargeable sensor nodes in the network. The computational complexity to find such a unique disk for a particular network deployment is $\mathcal{O}(N)$ [38]. Consequently, we have the following lemma on the search space of reader stop locations.

Lemma 1: To minimize the total charging delay for a network, the reader must stop within the SES C that covers all nodes in the network.

Proof: We prove this lemma by contradiction. Assuming there is an optimal stop location for the reader that is outside the SES area (denoted k in Fig. 3), then we could prove that there always exists a location within SES, which can lead to a smaller charging delay. Let the center of SES be O_C and h be the intersecting point where line segment $[k, O_C]$ cuts the SES circle. For any node i within SES, we have $d_{ih} < d_{ik}$, and consequently, $P_{ih} > P_{ik}$. Therefore, by relocating the reader from location k to h, we can always increase the charging power for any node i and reduce the charging delay at node i. Consequently, we prove k is not possible to be an optimal stop location for the reader, and this concludes the proof. ■

C. Discretizing Charging Power Within SES

Based on Lemma 1, we reduce the search space of reader stop locations from a 2-D space to a smaller enclosing circular area

C. However, the number of the potential reader stop locations within the SES C is still infinite, and we still cannot effectively apply the LP method in Section III-A to find out the optimal reader stop locations and the corresponding stop duration. Here, we adopt a novel method that was introduced by Shi and Hou [30] to divide the SES into a limited number of regions, and we represent each region by a charging power approximation vector. This discretization and region representation approach reduces the computational complexity significantly by only considering a limited number of potential regions for reader stop locations and guarantees near-optimal performance.

As the search space for potential stop locations is reduced to SES, the distance between node i in the network and the potential stop locations of the reader is also reduced to a limited range. Let O_C and R_C be the center and the radius of the SES disk C and D_{i,O_C} be the distance from node i to O_C; we can express the minimal and maximal distances from node i to all possible reader stop locations as

$$D_i^{\min} = 0 \tag{7}$$

$$D_i^{\max} = D_{i,O_C} + R_C. \tag{8}$$

With this range of charging distances and the charging model in (5), we can obtain the corresponding charging power range as

$$P_i^{\min} = \alpha / \left(D_{i,O_C} + R_C + \beta\right)^2 \tag{9}$$

$$P_i^{\max} = \alpha / \beta^2. \tag{10}$$

To discretize charging power within SES at node i, we divide SES C with respect to node i by drawing G_i number of concentric circles centered at node i with increasing radius of $D_i[1], D_i[2], \ldots, D_i[G_i]$, such that the difference of charging power between neighboring circles is less than a threshold value $\varepsilon (0 < \varepsilon < 1)$. Consequently, for a region between a pair of neighboring circles, the ratio difference of charging powers to node i is less than the threshold ε and can be represented by a discretized charging power sequence $P_i[1], P_i[2], \ldots, P_i[G_i]$, where $P_i[g]$ is

$$P_i[g] = P_i^{\max}(1+\varepsilon)^{-g} \quad (1 \le g \le G_i). \tag{11}$$

Fig. 4 visualizes the charging power discretization process by taking node 4 as an example. Combined with (11), when the reader stops on the circle of $D[1]$, the charging power to node 4 is $P_4[1] = P_4^{\max}(1+\varepsilon)^{-1}$, and $D[2]$ with $P_4[2] = P_4^{\max}(1+\varepsilon)^{-2}$. Hence, for the region between $D[1]$ and $D[2]$, the charging power is bounded by $P_4^{\max}(1+\varepsilon)^{-1}$ and $P_4^{\max}(1+\varepsilon)^{-2}$, with a difference of charging power to node 4 is less than the threshold ε.

The total number of concentric circles G_i for node i therefore is determined by the smallest circle, which is centered at node i and covers the whole SES C. In other words, G_i is the smallest integer number that satisfies the following condition: $P_i[G_i] = P_i^{\max}(1+\varepsilon)^{-G_i} \le P_i^{\min}$. Consequently,

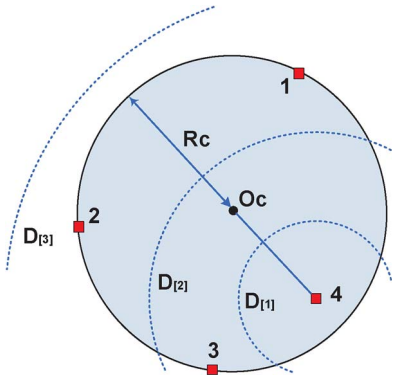

Fig. 4. Sequence of concentric circles with discretized charging power with origin of node 4.

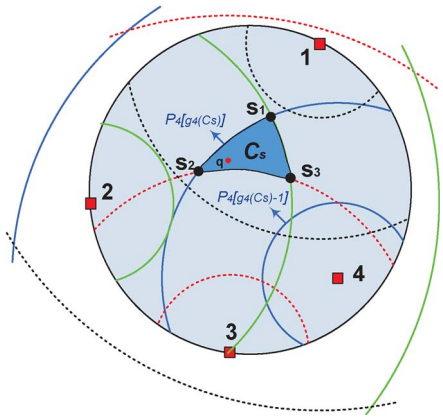

Fig. 5. Example of discretized charging regions within SES disk C.

combined with (9) and (10), we can determine G_i from the following:

$$G_i = \left\lceil \frac{\ln\left(\frac{P_i^{\max}}{P_i^{\min}}\right)}{\ln(1+\varepsilon)} \right\rceil = \left\lceil \frac{2\ln\left(1+\frac{1}{\beta}\left(D_{i,O_C}+R_C\right)\right)}{\ln(1+\varepsilon)} \right\rceil. \tag{12}$$

As Fig. 4 shows, $D_4[3]$ is the smallest circle centered at node 4 and covers the whole SES disk, and we have $G_4 = 3$.

Similarly for all nodes in the network, we can apply the same charging power discretization process on the SES and obtain a finite number of regions that are bounded by concentric circles. Such concentric circles are originated from all nodes in the network. The total number of regions, which are denoted as S, can be determined as follows. Each region's boundaries are determined by the circle of SES disk C and the concentric circles centered at all nodes. The largest number of the concentric circles within SES for each node i is $G_i - 1$, and there is only one SES disk circle; therefore, the total number of arcs within SES is $Z = 1 + \sum_{i \in N}(G_i - 1)$. By [39], the largest number of S, which is determined by Z arcs, has an upper bound, i.e.,

$$S \le Z^2 - Z + 2.$$

As an example, Fig. 5 shows the concentric circles that are originated from four nodes in the network and divide the whole SES into 28 different regions.

For each region, denoted as C_s (an example is shown in Fig. 5), the charging power difference from any location within this region to a neighboring region for all nodes in the network is bounded by the threshold value ε. For any region C_s, it must be within the arc with a radius of $D_i[g]$ that originates from node i, and we denote the sequence number of this arc (with respect to node i) as $g_i(C_s)$. Then, for any location $q \in C_s$, we have its charging power to node i as

$$P_i\left[g_i(C_s)\right] \leq P_i[q] \leq P_i\left[g_i(C_s)-1\right]. \tag{13}$$

Fig. 5 shows such an example. For any location q in the region C_s, its charging power to node 4 is $P_4[q]$, and we have $P_4[g_4(C_s)] \leq P_4[q] \leq P_4[g_4(C_s)-1]$ (in this example, $g_4(C_s)=2$). Since $(P_i[g_i(C_s)-1]/P_i[g_i(C_s)]) = 1+\varepsilon$ by (11), $P_i[q]$ has very tight lower and upper bounds of charging power with respect to node i.

Furthermore, for all N nodes in the network, within a region C_s, the charging power levels from any location in C_s to all nodes are also bounded and can be represented as an N-tuple charging power approximation vector $E_s = [P_1(C_s), P_2(C_s), \ldots, P_N(C_s)]$, where the ith element is

$$P_i(C_s) = P\left[g_i(C_s)\right]. \tag{14}$$

Fig. 5 shows an example, i.e., the charging power approximation vector for the region C_s (enclosed by arcs s_1, s_2 and s_3) is $[P_1(C_s), P_2(C_s), P_3(C_s), P_4(C_s)] = [P[2], P[2], P[3], P[2]]$, where the ith element in the vector is the lower charging power bound from any point in this region to node i. For any point $q \in C_s$ and its corresponding charging power approximation vector E_s, we have

$$P_i(C_s) \geq \frac{P_i(q)}{(1+\varepsilon)}. \tag{15}$$

Consequently, all such regions within SES can serve as a finite number of potential reader stop locations and use the LP method to solve (3) in Section III-A. The optimal total stop duration obtained by the LP method after discretization has a $1/(1-\varepsilon)$ approximated ratio to the theoretically optimal charging delay. The detailed proof is provided in the Appendix, and we further verify this approximated ratio through extensive evaluations in Section V.

D. Reader Stop Location Merging Design

After charging power discretization in Section III-C, we reduce the search space for the LP formulation in Section III-A from infinite space to a finite number of potential reader stop locations. However, the optimal charging delay obtained may consist of a large number of reader stop locations. For example, Fig. 6(a) shows a random deployment with 200 nodes and the corresponding optimal reader stop locations (denoted by stars in the figure). From Fig. 6(a), we can see the reader has to stop at a very large number of locations (159 in this specific example) to achieve the optimal charging delay. However, for real-world applications, it is not very practical to move the reader among a large number of stop locations. Therefore, here, we introduce a reader stop location merging design that effectively reduces the number of stop locations for the reader while maintaining the charging delay increase within a specified threshold.

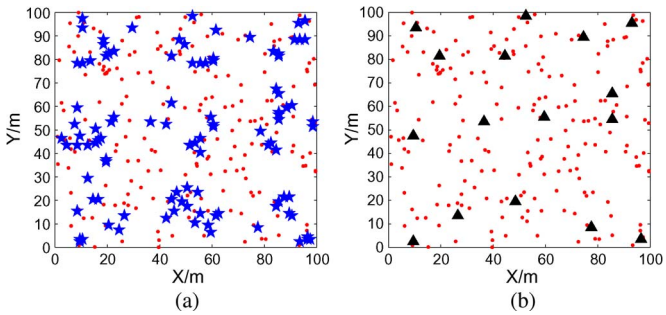

Fig. 6. Reader stop locations before and after merging (sensor node marked as circular dots). (a) Reader stop locations before merging (marked as stars). (b) Reader stop locations after merging (marked as triangular dots).

To merge these reader stop locations in the previous results, we use a well-known k-means clustering algorithm, known as Lloyd's algorithm [40], to group reader stop locations into multiple clusters based on their geographical locations. Lloyd's algorithm is a method of cluster analysis, which aims to partition the n observations into k clusters in which each observation belongs to the cluster with the nearest mean. Li *et al.* [41], [42] proposed distributed clustering algorithms based on an information theoretic measure, to present linear- and kernel-distributed clustering algorithms, and achieve better performance since they take the whole distribution of cluster data into account.

For our reader stop location merging problem, the original n observations in the Lloyd's algorithm is simply the total number of reader stop locations obtained using charging power approximation vectors in Section III-C. However, for the number of clusters to be formed (k in the Lloyd's algorithm), it is not obvious how to determine a suitable value. Therefore, in our reader stop location merging design, instead of asking system users to specify the k value, we request system users to determine how much performance degradation they could tolerate to reduce the number of reader stop locations. Specifically, we let the system users to specify a threshold value θ, such that the charging delay before stop location merging T_{before} and after merging T_{after} satisfy the following:

$$\left|\frac{T_{\text{after}} - T_{\text{before}}}{T_{\text{before}}}\right| \leq \theta. \tag{16}$$

Essentially, θ determines the percentage of charging delay increase that the merging design can tolerate with respect to the delay before merging. Consequently, the charging delay after merging has an upper bound $(1+\theta)T_{\text{before}}$.

After introducing the delay threshold value θ, the next question we need to answer is how to correlate θ with the number of clusters after merging (parameter k in the Lloyd's algorithm). To reveal the relationship between θ and charging delay after merging (T_{after}), we use Fig. 7 to demonstrate how the charging delay changes with different values of merging parameter k in the Lloyd's algorithm. From Fig. 7, we can see that, with the increasing number of stop location clusters from the Lloyd's algorithm, the charging delay decreases sharply when the

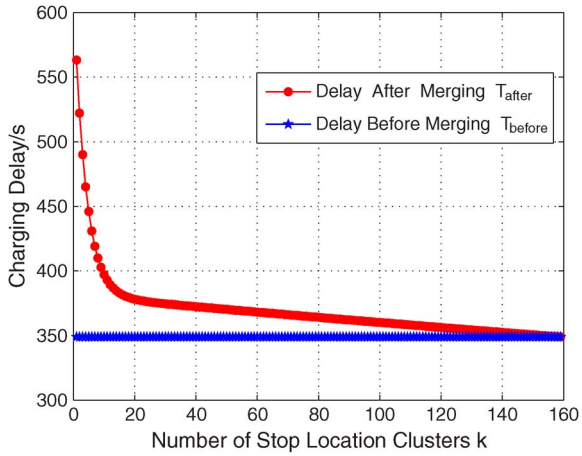

Fig. 7. Charging delay versus the number k of stop location clusters.

number of clusters after merging is small and decreases slowly and approaches to the original charging delay when the number of clusters after merging is getting larger. Since the charging delay monotonically decreases with respect to the number of merged clusters, we can perform binary search to find the minimal k value in the Lloyd's algorithm to satisfy the delay threshold θ.

After obtaining the optimal k value, we then need to select one representative stop location within each of the k clusters. To select such a representative stop location within a cluster, we pick a location whose charging power vector is closest to the average charging power vector within this cluster. Specifically, assuming a cluster contains M original reader stop locations, and their corresponding power vector is $E_1, E_2, \ldots, E_M$, respectively, we choose the representative location whose charging vector E_i satisfies

$$E_i = \arg\min_{E_i \in E} \left(\left\| E_i - \left(\sum_{j=1}^{M} E_j \right) \Big/ M \right\|_2 \right). \tag{17}$$

Fig. 6(b) shows an example of reader stop locations after merging. If given a delay threshold $\theta = 0.1$, we perform binary search to find the minimal k value in the Lloyd's algorithm to satisfy that this delay threshold is $k = 16$. Then, we select one representative stop location within each of the k clusters by (17) and mark these 16 representative locations as triangle dots in Fig. 6(b). Consequently, the charging delay after merging has an upper bound $(1+\theta)T_{\text{before}} = 1.1T_{\text{before}}$.

E. Putting all Things Together

To summarize our design, we divide it into following four main steps:

1) finding the SES that covers all nodes in the network;
2) discretizing SES by charging power for all nodes in the network;
3) solving (3) with discretized SES regions using LP methods, obtaining approximated optimal locations;
4) merging these original approximated optimal locations into a smaller number of locations with a delay upper bound.

The approximation ratio for our design is $(1+\theta)/(1-\varepsilon)$ to the theoretically optimal charging delay.

The computation complexity of our design is determined by adding the following three parts. The first one (see Section III-B) for finding the SES disk is $\mathcal{O}(N)$ [38]. The second one (see Section III-C) for performing the LP method to find approximated optimal locations is determined by the total number of partition regions, whose number has an upper bound as analyzed at the end of Section III-C. Hence, combined with (12), we obtain: $\mathcal{O}(Z^2) = \mathcal{O}((\sum_{i\in N} G_i)^2) = \mathcal{O}((N/\varepsilon)^2)$. The third part (Section III-D) is determined by the number of iterations of performing LP method to find the minimal k value using binary search ($\mathcal{O}(\log N)$ by [43]). As the complexity of the Lloyd's algorithm in each step of binary search is $\mathcal{O}(N)$ [40], the complexity of the third part is $\mathcal{O}(N \log N)$. Therefore, the total computation complexity of our design is $\mathcal{O}((N/\varepsilon)^2)$.

IV. Practical Issues

A. Sensor Nodes Deployed With Location Uncertainty

After obtaining the optimal solution, here, we consider a practical issue that the sensor nodes are deployed with location uncertainty. Many existing works in wireless sensor networks assume the knowledge of exact locations of sensor nodes. In practice, however, this assumption is not always valid as location uncertainty in actual sensor deployment exists [32]–[34]. For instance, sensor node with onboard GPS has an accuracy of three meters on average by recent technology [44]. Even carefully positioned in the deployment phase, sensor nodes may be displaced due to environmental or human factors during the course of operation. Further, uncertainty of sensor locations may also arise from privacy or security concerns. Given the uncertainty in sensor node location, we investigate to which degree our design can tolerate the location error here.

We first theoretically investigate the maximal value of location uncertainty that our method can tolerate by analyzing the average region size after the discretization process. We take one sensor node case as an example to illustrate, and the result of the multiple-node case is provided in Section V-E. To find the degree to which our method can tolerate location uncertainty, we analyze the distance between neighboring concentric circles after the discretization process. Let $L[g]$ be the distance value between two neighboring concentric circles $D[g]$ and $D[g-1]$, such that $L[g] = D[g] - D[g-1]$. Fig. 8 visualizes an example of the $L[g]$ values for three circles. Then, we analyze how the g value influences $L[g]$. Combining $P[g] = P^{\max}(1+\varepsilon)^{-g}$ [see (11)] and $P[g] = \alpha/(D[g]+\beta)^2$ [see (2)], we obtain $P^{\max}(1+\varepsilon)^{-g} = \alpha/(D[g]+\beta)^2$. Therefore, we obtain $D[g] = \sqrt{(\alpha/P^{\max})(1+\varepsilon)^g} - \beta$, based on which, we further get

$$\begin{aligned} L[g] &= D[g] - D[g-1] \\ &= \sqrt{\frac{\alpha}{P^{\max}}} \left[\sqrt{(1+\varepsilon)^g} - \sqrt{(1+\varepsilon)^{g-1}} \right] \\ L[g-1] &= D[g-1] - D[g-2] \\ &= \sqrt{\frac{\alpha}{P^{\max}}} \left[\sqrt{(1+\varepsilon)^{g-1}} - \sqrt{(1+\varepsilon)^{g-2}} \right]. \end{aligned}$$

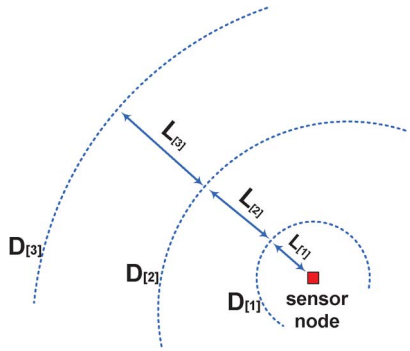

Fig. 8. Distance between neighboring concentric circles.

By subtracting the above two equations, we obtain that

$$\begin{aligned} &L[g]-L[g-1] \\ &= \sqrt{\frac{\alpha}{P^{\max}}}\cdot\left[\sqrt{(1+\varepsilon)^{g}}+\sqrt{(1+\varepsilon)^{g-2}}-2\sqrt{(1+\varepsilon)^{g-1}}\right] \\ &= \sqrt{\frac{\alpha}{P^{\max}}(1+\varepsilon)^{g-2}}\cdot\left[\sqrt{(1+\varepsilon)^{2}}-2\sqrt{1+\varepsilon}+1\right] \\ &= \sqrt{\frac{\alpha}{P^{\max}}(1+\varepsilon)^{g-2}}\cdot\left[\sqrt{1+\varepsilon}-1\right]^{2} \\ &> 0. \end{aligned}$$

This result means that $L[g]$, which is the distance between two neighboring concentric circles, becomes larger when the value of g increases. Therefore, the region enclosed by the smallest circle $D[g]$ is the most sensitive part for the location uncertainty. Hence, the smallest circle indicates the maximal tolerated location error, which is

$$L[1]=D[1]=\sqrt{\frac{\alpha}{P^{\max}}\cdot(1+\varepsilon)}-\beta \tag{18}$$

where α, β, and $P^{\max}$ are constant parameters depending on environment or system setting. The value of ε in (18) influences $L[g]$ and further the system sensitivity to location uncertainty. This property indicates that we can adjust the value of charging power discretization threshold ε to tolerate specified requirements of sensor node location error. We further verify this result through numerous simulations in Section V-E.

B. Optimal Reader Stop Sequence

Here, we design an optimal reader stop sequence after obtaining the stop locations. At the end of algorithm, as shown in Section III-D, we obtain the approximated optimal stop locations without considering their sequence. However, in system implementation, it is a practical issue to sequence their stops to achieve an optimal network charging performance, particularly when only one reader exists. Intuitively, sequencing the stop locations [Fig. 6(b) shows an example] to minimize the reader travel distance is an alternative. Consequently, this problem can be transformed to a typical traveling salesman problem (TSP). However, this problem is not the research scope of our work as we do not consider the charging action when reader traveling between any two stop locations. Here, we define another new metric to describe the optimal network charging performance and introduce the motivation for this consideration.

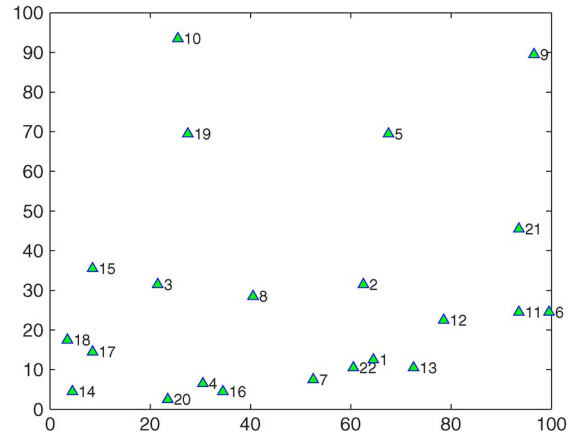

Fig. 9. Reader stops with a random sequence.

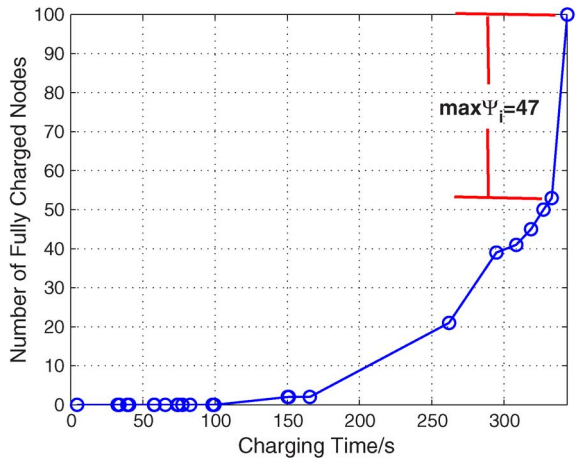

Fig. 10. Charging performance when reader stops with a random sequence.

In our design, the charged energy in the sensor nodes can be accumulated after each reader stop. Consequently, a certain reader stop sequence results in a unique temporal distribution of the number of fully charged nodes after each reader stop. Fig. 9 shows an example of a random sequence for the obtained 22 reader stop locations, with a number to indicate each stop sequence. Under this charging sequence, the corresponding charging performance is shown in Fig. 10, in which each dot indicates the number of fully charged nodes after each reader stops as Fig. 9 shows. We can see in Fig. 10 that the number of fully charged nodes during the last two reader stops has a sharp growth, which has 47 nodes in only 10.5 s. This charging explosion may incur heavy system overhead, such as communication interference [45]. Hence, it is beneficial to schedule optimally the reader stop order, the same as charging sequence, to achieve a steady charging performance in a smoother manner. To characterize such steady performance, we denote Ψ_i as the increased number of fully charged sensor nodes between the $i-1$th and ith reader stops. We define the maximum value of Ψ_i, denoted by $\max \Psi_i$ as a metric to indicate a steady charging performance, e.g., $\max \Psi_i = 47$ in Fig. 10. Obviously, a

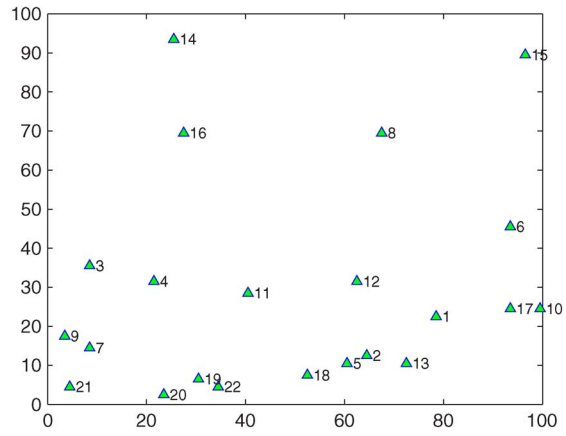

Fig. 11. Reader stops with an optimal sequence.

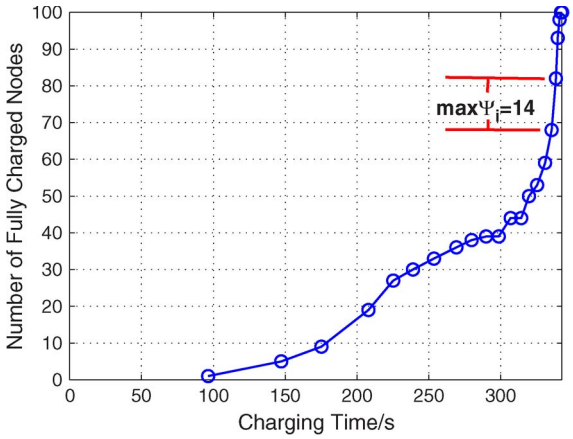

Fig. 12. Charging performance when reader stops with an optimal sequence.

bigger value of $\max \Psi_i$ means a larger probability for number explosion of fully charged sensor nodes. Therefore, our goal is to schedule the reader stop sequence to minimize the $\max \Psi_i$ value, i.e.,

$$\min(\max \Psi_i).$$

We can see that scheduling the reader stop sequence is the same as using a line to connect all the stop locations in Fig. 9, which is similar to a typical TSP problem. The TSP problem is $NP-hard$ and has high computation complexity [43]. For example, with k number of stop locations, it has computational complexity of $\mathcal{O}(k!)$ if we use an exhaustive search method to minimize $\max \Psi_i$. Since there is no algorithm to find the optimal sequence with low computation complexity, we provide a direct greedy method to solve this problem. In each ith scheduling step, we choose a reader stop location that results in a minimal Ψ_i value. We use this greedy method to reorder the reader stop sequence as shown in Fig. 11, which has a charging performance, as Fig. 12 shows. This result has a more steady performance as $\max \Psi_i$ reduces from 47 to 14. By comparing with Fig. 10, we can see in Fig. 12 that this improved charging sequence has a smoother charging process without any sharp growth. It is worthy to notice that this heuristic method only has computation complexity of $\mathcal{O}(k^2)$.

V. Evaluation

Here, extensive simulations are conducted to evaluate our design under different network settings and reveal insights of system performance.

A. Simulation Setup

We assume that wireless rechargeable sensor nodes are randomly deployed over a 100 m $\times$ 100 m 2-D square area. The default number of sensor nodes is 100. For the charging model [see (2)], we set $\alpha = 36$ and $\beta = 30$, which are obtained by fitting of our experiment curve as mentioned in Section II-B. The charging power discretization threshold value is $\varepsilon = 0.05$, and the stop location merging threshold is $\theta = 0.05$. For each node, the energy threshold to function properly is 2 J, which is essential for the WISP node to preform several sensing and computing tasks [23].

Each point in simulation figures is obtained by averaging 100 runs with different random seeds and node deployments.

B. Baseline Setup

Since there is currently no existing works that are designed to minimize charging delay in wireless rechargeable sensor networks, to compare the system performance of our design, we introduce a baseline design that utilizes the concept of set cover [46]. Essentially in this baseline design, the RFID reader tries to maximize the number of undercharged nodes in its surrounding region at individual stops.

In addition to the baseline design above, we also obtain the minimal charging delay by the fine-grained exhaustive search using the LP formulation in (3). This baseline is used to demonstrate the performance gap between our design and the theoretical charging delay lower bound.

C. Performance Comparison

Here, we show the system performance under various designs with different system parameters, including the charging power discretization threshold ε, stop location merging threshold θ, the number of nodes, and onboard capacitor size of node.

1) Impact of Charging Power Discretization Threshold ε: As discussed in Section III-C, the charging power discretization threshold ε affects the gap between the optimal charging delay and our approximated minimal delay with significantly reduced computational overhead. Therefore, we investigate the charging delay under different charging power discretization threshold values ε. As shown in Fig 13, the charging delay remains constant for the optimal solution and baseline design as they are not affected by the charging power discretization threshold. In contrast, the charging delay of our approximated optimal design and stop location merging design increase with the increasing threshold value ε. This is because, with a larger ε value, the charging power vectors at individual discretized regions within SES become less bounded and, consequently, lead to longer charging delays with such larger charging power errors.

On the other hand, the charging power discretization threshold ε also affects the computational overhead of our design

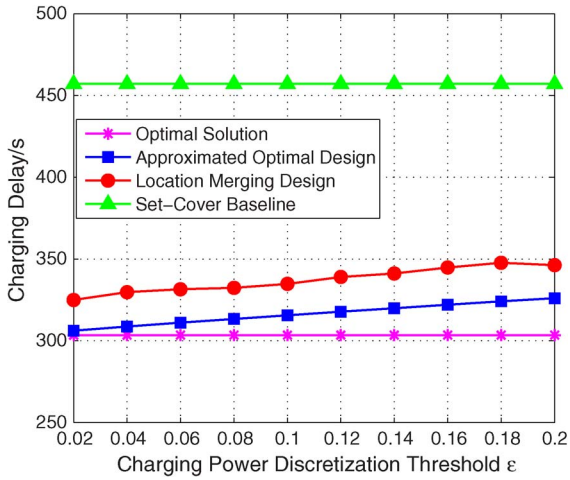

Fig. 13. Delay versus charging power protect discretization threshold ε.

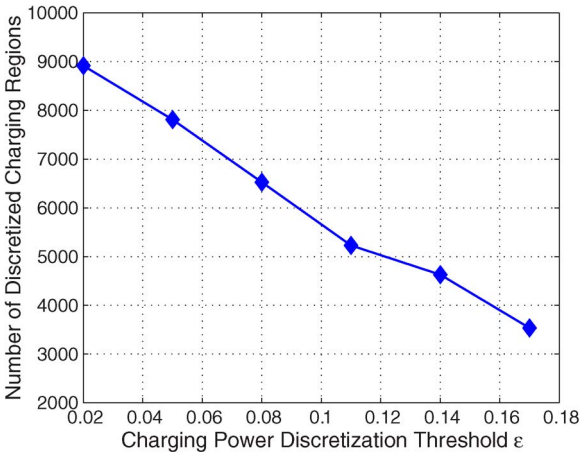

Fig. 14. Number of discretized regions versus threshold ε.

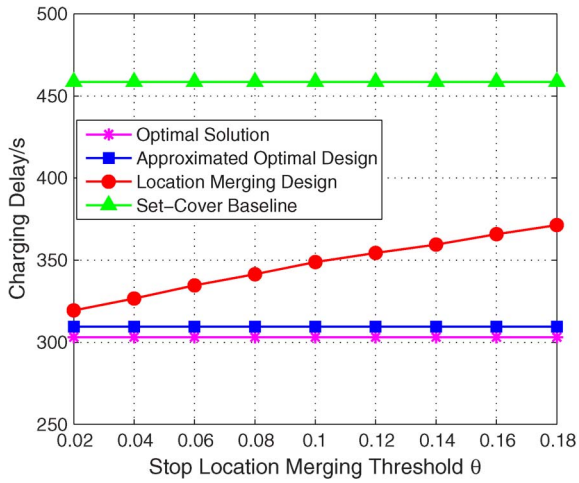

Fig. 15. Delay versus stop location merging threshold θ.

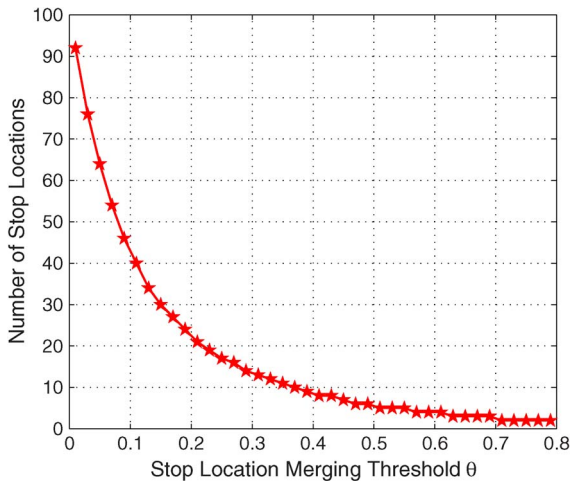

Fig. 16. Reader stop location number versus merging threshold θ.

as analyzed in Section III-E. To visualize such computational overhead, Fig. 14 shows the number of discretized charging regions under different charging power discretization threshold values. As shown in Fig. 14, the number of discretized charging regions decreases with the increasing charging power discretization threshold values, which in turn decreases the computational complexity as the number of potential reader stop locations decreases. For example, when ε increases from 0.02 to 0.17, the number of discretized charging regions decreases by 60.34%. Therefore, based on the tolerable error range for the system, we can select an appropriate ε value to reduce the computational overhead while satisfying the system requirements.

To compare with the baseline solutions, we can see that the charging delays of our stop location merging design outperforms the set-cover-based baseline design at all charging power discretization threshold values. On average, our stop location merging design has 26.42% charging delay deduction when compared with the set-cover-based baseline design.

Furthermore, our design in Section III-D aims to ensure that the obtained charging delay has an approximation ratio of $(1+\theta)/(1-\varepsilon)$ with respect to the charging delay of optimal solution. In Fig. 13, we also show that the charging delays of our design validate this approximation ratio. For example, when $\varepsilon = 0.1$, the optimal delay is 303.4 s, and the delay upper bound value is $((1+0.05)/(1-0.1)) \times 303.4\,\text{s} = 354.0\,\text{s}$ $(\theta = 0.05)$. At the same threshold value, the actual charging delay of our stop location merging design is 334.8 s, which therefore satisfies the delay bound.

2) Impact of Stop Location Merging Threshold θ: Here, we study the impact of reader stop location merging threshold θ on the charging delays. In Section III-D, we introduce the stop location merging scheme to reduce the number of reader stop locations for practical systems, and θ is used to control the charging delay bound. Fig. 15 shows the charging delays of different designs under varying θ values. In Fig. 15, we can see that charging delays for the stop location merging design increase almost linearly with the increasing θ value, whereas all other designs are not affected and remain constant. However, even when $\theta = 0.18$, the charging delay of our stop location merging design still outperforms the set-cover-based design by 19.03%. On average, our stop location merging design has 24.7% charging delay deduction when compared with the set-cover-based design.

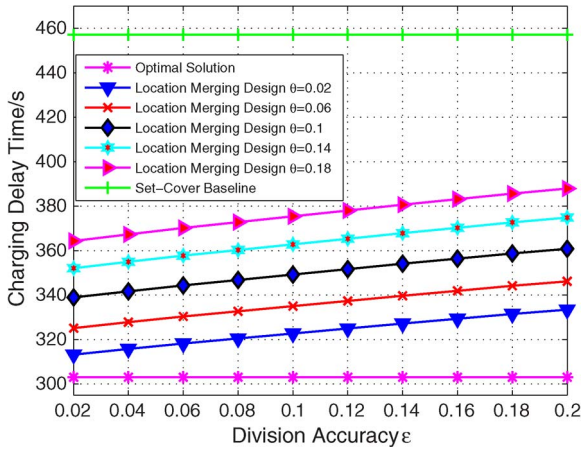

Fig. 17. Stop location merging threshold θ versus charging power discretization threshold ε.

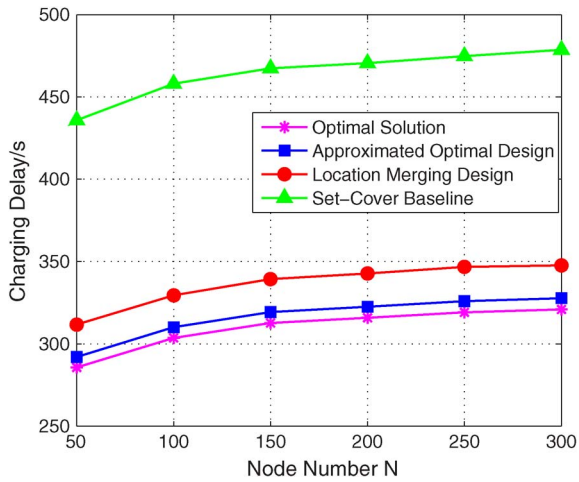

Fig. 18. Charging delay versus node number.

To demonstrate the effectiveness of our stop location merging design, we also show the change of the number of reader stop locations under different θ values in Fig. 16. With an increasing value of θ, the number of stop locations decreases sharply. Combined with the analysis of Figs. 15 and 16, our stop location merging design can significantly reduce the number of stop locations with a slight delay increase.

We show the performance by simultaneously varying the stop location merging threshold θ and charging power discretization threshold ε in Fig. 17. A designer can choose appropriate values for these parameters according to his requirement.

3) Impact of Node Number: We study the scalability of our design and investigate the charging delays with a varying number of nodes in the network. Fig. 18 shows the impact of node density on the system performance. As the node density increases, the charging delays of all solutions also increase because there are more nodes needing to be charged. However, under all node density settings, it can be found that our designs significantly outperform the set-cover-based baseline design and closely approximate the optimal charging delay. For example, when the number of nodes is 200 in the network, the charging delays for the optimal solution, approximated optimal design, stop location merging design and set-cover-based design are 312.7, 319.3, 339.4, and 467.4 s, respectively. Based on the delay of the optimal solution, we calculate the delay upper bound with approximation ratio as $((1+\theta)/(1-\varepsilon)) \times 312.7$ s $= 345.6$ s, and we can see that the delay of our stop location merging design still satisfies this bound.

4) Impact of Varying Charging Models: We are interested in investigating the impact of different charging model parameters on the system performance. In particular, we study the impact of varying onboard capacitor sizes on the network charging delays, which can provide guidance for the system designers when choosing appropriate capacitor size for their nodes. To simplify the description, we use the default charging delay T_0, which is defined as the charging time for the node when the charging power is maximal (right next to the RFID reader), to represent different onboard capacitor sizes. Fig. 19 shows the charging delay under different default charging delays T_0, which corresponding to different onboard capacitor sizes. From

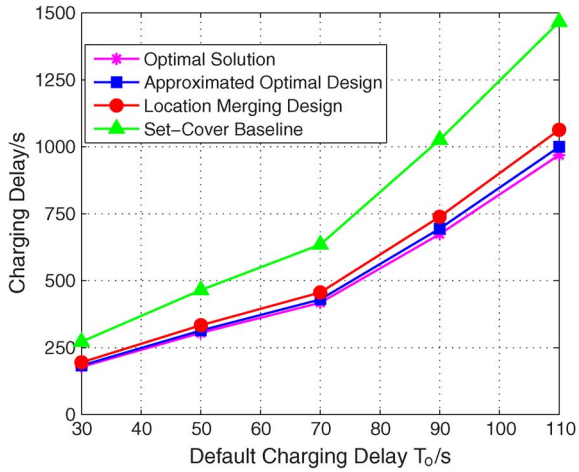

Fig. 19. Delay versus default charging delay.

Fig. 19, we can see that our designs outperform the set-cover-based baseline design under all default charging delays. As T_0 becomes larger, the performance difference between our designs and set-cover design also becomes larger. For example, when the default charging delay is $T_0 = 30$ s, the difference between stop location merging design and set-cover baseline is 76.9 s, whereas when the default charging delay is $T_0 = 110$ s, the corresponding difference is 404.1 s. This increasing gap of charging delays is because with a larger default charging delay T_0, each individual node needs more time to charge on average. As our stop location merging design provides a higher charging efficiency so that the total charging delay can be reduced more significantly.

D. System Insights

To reveal the insight about why our proposed design can significantly reduce charging delay, we conduct a simulation to observe the energy level on each node after charging with four solutions. Intuitively, the charging efficiency is high if each individual node is charged just with exact energy threshold 2 J. The energy level for each node after charging is shown in Fig. 20. We can see that in top two subfigures of Fig. 20, most

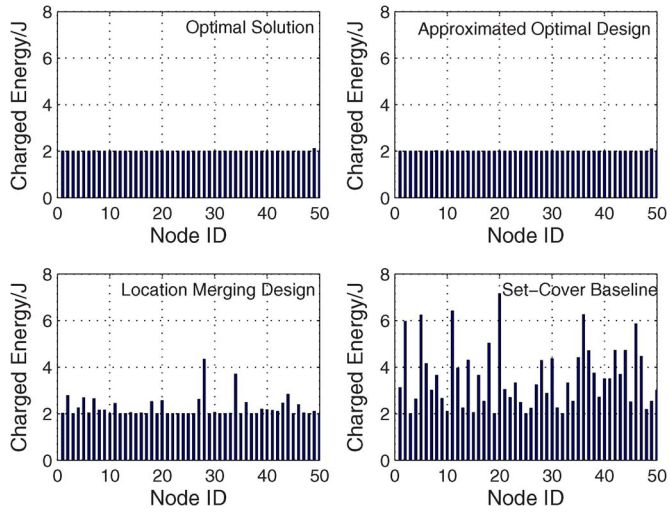

Fig. 20. Energy levels after charging with four solutions.

nodes exactly have levels of energy threshold; therefore, the charging efficiency is high, and a short charging delay is obtained. Comparing the bottom two subfigures, the energy level of set-cover baseline has a more various distribution, even many nodes are charged above 4 J. Hence, a lot of energy is wasted by this charging solution and incurs low charging efficiency. On the contrary, our stop location merging design charges energy to the nodes in a more balanced manner; therefore, the charging efficiency is improved, and our design can reduce charging delay significantly.

E. Performance With Sensor Deploy Uncertainty

To verify whether our design can tolerate sensor node location error as Section IV-A mentioned, we conduct simulation to reveal performance of our design. We first obtain the approximated charging strategy by our design, which is based on the sensor networks deployed with location uncertainty. This strategy includes approximated optimal reader stop locations and corresponding stop duration. Then, we use this stop strategy to charge the actual sensor network, which is with ground-truth locations, to record how many nodes are charged above energy threshold after charging. We set the ratio of fully charged nodes to total number of nodes as the y-axis in Fig. 21, under varying average location error as x-axis. Every point in this figure is obtained by averaging 100 runs, and the variance of each point is also provided. Fig. 21 shows that our design can guarantee most nodes are fully charged, e.g., 94.5% nodes are charged above energy threshold with an average location error of 3 m. Moreover, even with average location error of 6.4 m, our method can charge 89.1% nodes with full energy. Further, we can see in Fig. 21 that all the sensor nodes can be fully charged when the average location error is smaller than 0.8 m. As the typical localization error has a decimeter scale [47]; therefore, our solution can work in these practical settings.

Fig. 22 shows fully charged node ratio under varying values of charging power discretization threshold ε and setting the average location error as 3 m. We can see in Fig. 22 that the charged ratio curve has a positive correlation with the ε value. This result coincides with our design property that a

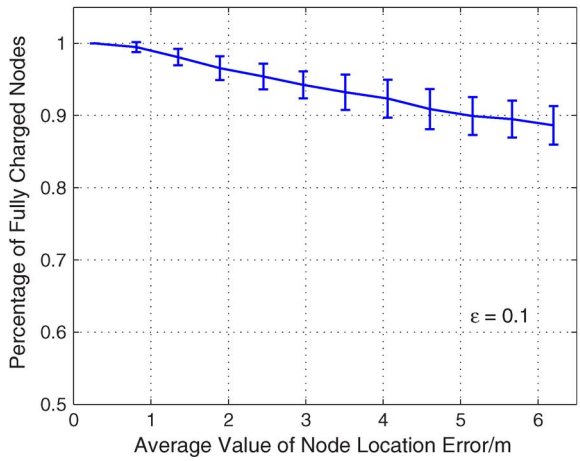

Fig. 21. Charged ratio versus average value of node location error, with $\varepsilon = 0.1$.

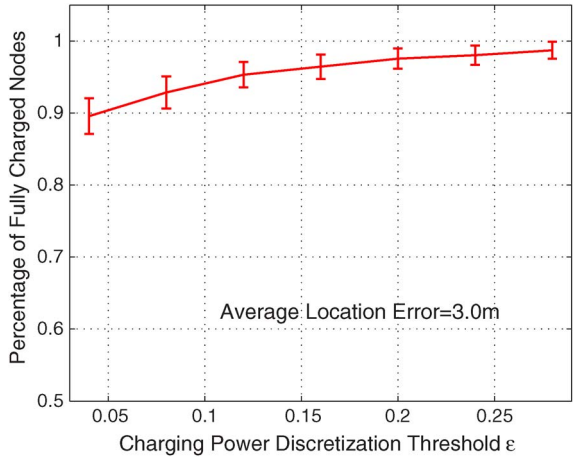

Fig. 22. Charged ratio versus charging power discretization threshold ε.

larger ε value indicates a larger average discretized region and, consequently, enable our design to tolerate bigger average location error.

Based on given two results, we are interested in investigating the maximal average tolerated location error under a certain value of charging power discretization threshold ε. Fig. 23 shows such simulation results as the curve has a positive correlation with increasing ε values. This curve trend coincides with our design property as described earlier and verifies the theoretical analysis in Section IV-A. Combined with the results of Figs. 13 and 23, we can see that a bigger value of ε results in slightly long charging delay but enables our design to tolerate larger location error of sensor deployment. Hence, there is a tradeoff between location error tolerance and charging delay under varying ε values. Inspired by this property, in practical system implementation, we can carefully adjust the values of ε to satisfy different user requirements.

VI. Related Work

Recently, much research has focused on improving charging efficiency in wireless rechargeable sensor networks. In general, these works can be classified into two categories: hardware design and network charging coordination.

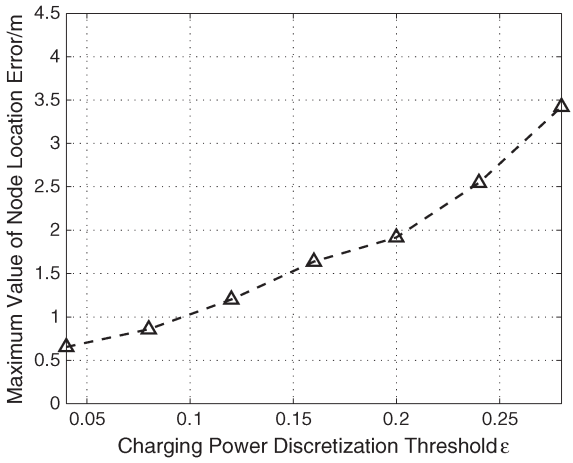

Fig. 23. Maximum value of node location error versus charging power discretization threshold ε.

Many pioneer works have focused on hardware design to improve charging efficiency [20]–[22]. Kurs *et al.* [48] experimentally showed that the overall output efficiency of charging multiple devices is larger than the output efficiency of charging each device individually by designing an enhanced technology. Sample *et al.* [23] designed a scheme of analog circuitry for the WISP node to obtain an efficient conversion of the incoming RF energy. Liu *et al.* [4] designed a new communication system that enables two devices to communicate using ambient TV signals as the only source of power, and they introduce a more energy-efficient ambient backscatter as a communication method. Different from the hardware design, this paper is focused on intranetwork optimization, and the increase in charging efficiency originated from a hardware domain could simultaneously improve the performance of our design.

From the view of networks, some recent works have investigated the network charging coordination to improve charging performance. He *et al.* [49] considered the static reader deployment in a wireless rechargeable sensor networks so that the nodes can harvest enough energy for continuous operation. In [50], Xie *et al.* considered a similar charging scenario by jointly designing the flow routing among the network and the charging time of the wireless charging vehicle at each stop point and propose a near-optimal solution with guaranteed accuracy. The difference between their work and ours lies in the fact that they consider the case where all the stop locations are discrete, and we consider a situation where potential stop locations constitute a continuous area. Therefore, their results cannot be applied to our problem. We propose a new scheme to simultaneously find the optimal reader stop locations and the corresponding stop duration. He *et al.* [51] proposed a novel energy synchronized charging protocol to simultaneously reduce both the charger travel distance and the charging delay of sensor nodes. However, their design requires that the charger should replenish energy via short-distance or direct-contact charging technologies, which means the charger charges energy to the node one by one. In [52], a proof-of-concept prototype of wireless charging system for sensor networks and conduct experiments was built to evaluate its feasibility and performance in small-scale networks. Bin *et al.* [53] investigated how to minimize charging cost by reducing energy consumption rate and improving recharging efficiency. In this paper, our key objective is to minimize the charging delay for the whole network, which is fundamentally different from most existing works.

VII. Conclusion

We studied a general scenario of randomly deployed sensor nodes, where a reader moving as a point way in the network and staying for some duration at each location, respectively, to charge energy to the nodes. We proposed a solution to find the optimal set of stopping locations to achieve an approximated minimum of total charging time cost with low search complexity. Specifically, we first narrowed the search space into a smallest enclosed disk and further divided this disk into a finite number of regions with an accuracy value of ε. Then, we presented each region with a charging power vector and used the LP method on these regions to find the optimal set of regions to position the reader with corresponding staying time. For practical consideration, we further proposed a location merging design to merge original stop locations into a smaller number with a delay upper bound. The total delay cost obtained by our design was $(1+\theta)/(1-\varepsilon)$ to the theoretically optimal one. We provided detailed illustration for the designs in simulation, which achieved an approximated result with low search complexity. We also made guidelines for reader stopping locations to minimize total delay cost. This solution could be used in other energy harvesting scenarios, with different types of sensor platforms or energy sources.

Appendix
Approximation Ratio Proof

Here, we prove that the optimal total stop duration obtained by LP method after discretization has a $1/(1-\varepsilon)$ approximated ratio to the theoretically optimal charging delay under the condition that the reader only stops once. For a more general case, when the reader has multiple stops, we verify the approximated ratio through extensive evaluations in Section V.

Denote $q_{\rm opt}$ as the theoretically optimal reader stop position (unknown), and $T_{\rm opt}$ and $E_{\rm opt}$ as the corresponding minimum charging delay and charging power vector, respectively, all of which are unknown. We denote E^* as the optimal one among all charging power approximated (CPA) vectors E_s, $s=1,2,\ldots,S$ to obtain minimum charging delay, which delay is denoted as T^*; therefore, $T^*=\min(T_s: s=1,2,\ldots,S$.

Theorem 1: For any reader stopping position q with its corresponding charging power vector E and optimal minimum charging delay T, denote C_s as the region covering q for a given $\varepsilon>0$. Then, we calculate E_s for this C_s and claim its corresponding achievable optimal minimum charging delay T_s (via LP method) as $T_s \le T/(1-\varepsilon)$.

Proof: Instead of using the optimal charging power vector E_s for C_s, we use charging power vector E to represent CPA vector of this region, which is obviously suboptimal. We denote $\hat{T}_s$ as the minimum delay obtained for C_s under E; therefore, $T_s \le \hat{T}_s$. Then, we only need to prove $\hat{T}_s \le T/(1-\varepsilon)$. To

prove this, combined with (4), we calculate the total energy charged on node i at time $T/(1-\varepsilon)$, which is

$$P_i \cdot T/(1-\varepsilon) > P_i \cdot T \geq \delta.$$

The last inequality holds by the energy constraint in charging power vector for point q. Then, the minimum delay $\hat{T}_s$ for subarea C_s under E is at most $T/(1-\varepsilon)$, and we have $T_s \leq \hat{T}_s \leq T/(1-\varepsilon)$. ■

Theorem 2: With aforementioned T^* and $T_{\rm opt}$, we have $T^* \leq T_{\rm opt}/(1-\varepsilon)$.

Proof: Consider a special case of Theorem 1 that a given reader stopping position is the theoretically optimal one $q_{\rm opt}$, with corresponding $E_{\rm opt}$ and $T_{\rm opt}$. Using the similar proof process, denote C_s as the region covering $q_{\rm opt}$ with corresponding E_s; then, we obtain $T_s \leq T_{\rm opt}/(1-\varepsilon)$. Hence, for the optimal E^* among all the CPA vectors, we have $T^* \leq T_s \leq T_{\rm opt}/(1-\varepsilon)$. The proof is completed, and this theorem guarantees that the minimum optimal charging delay among all the S CPA vectors is at most $T_{\rm opt}/(1-\varepsilon)$. ■

REFERENCES

[1] L. Fu, P. Cheng, Y. Gu, J. Chen, and T. He, "Minimizing charging delay in wireless rechargeable sensor networks," in *Proc. IEEE INFOCOM*, 2013, pp. 2922–2930.

[2] S. He *et al.*, "Energy provisioning in wireless rechargeable sensor networks," *IEEE Trans. Mobile Comput.*, vol. 12, no. 10, pp. 1931–1942, Oct. 2013.

[3] L. He *et al.*, "Evaluating service disciplines for on-demand mobile data collection in sensor networks," *IEEE Trans. Mobile Comput.*, vol. 13, no. 4, pp. 797–810, Apr. 2014.

[4] V. Liu *et al.*, "Ambient backscatter: Wireless communication out of thin air," in *Proc. IEEE SIGCOMM*, 2013, pp. 39–50.

[5] D. Takaishi, H. Nishiyama, N. Kato, and R. Miura, "Towards energy efficient big data gathering in densely distributed sensor networks," *IEEE Trans. Mobile Comput.*, vol. 2, no. 3, pp. 388–397, Sep. 2014.

[6] L. He *et al.*, "Mobile-to-mobile energy replenishment in mission-critical robotics sensor networks," in *Proc. IEEE INFOCOM*, 2014, pp. 1195–1203.

[7] S. Zhang, J. Wu, and S. Lu, "Collaborative mobile charging," *IEEE Trans. Comput.*, vol. 64, no. 3, pp. 654–667, Feb. 2015.

[8] H. Dai *et al.*, "Quality of energy provisioning for wireless power transfer," *IEEE Trans. Parallel Distrib. Syst.*, vol. 26, no. 2, pp. 527–537, Feb. 2015.

[9] D. Niyato and P. Wang, "Delay-limited communications of mobile node with wireless energy harvesting: Performance analysis and optimization," *IEEE Trans. Veh. Technol.*, vol. 63, no. 4, pp. 1870–1885, May 2014.

[10] X. Lu, P. Wang, D. Niyato, and E. Hossain, "Dynamic spectrum access in cognitive radio networks with RF energy harvesting," *IEEE Wireless Commun.*, vol. 21, no. 3, pp. 102–110, Jun. 2014.

[11] D. Niyato, P. Wang, and D. I. Kim, " Performance analysis and optimization of tdma network with wireless energy transfer," *IEEE Trans. Wireless Commun.*, vol. 13, no. 8, pp. 4205–4219, Aug. 2014.

[12] A. Liu, X. Jin, G. Cui, and Z. Chen, "Deployment guidelines for achieving maximum lifetime and avoiding energy holes in sensor network," *Inf. Sci.*, vol. 230, pp. 197–226, May 2013.

[13] C. Huang, R. Zhang, and S. Cui, "Throughput maximization for the Gaussian relay channel with energy harvesting constraints," *IEEE J. Sel. Areas Commun.*, vol. 31, no. 8, pp. 1469–1479, Jul. 2013.

[14] D. Shin, S. He, and J. Zhang, "Robust, secure, and cost-effective design for cyber-physical systems," *IEEE Int. Syst.*, vol. 29, no. 1, pp. 66–69, Jan./Feb. 2014.

[15] Z. Wang, J. Liao, Q. Cao, and H. Qi, "Achieving k-barrier coverage in hybrid directional sensor networks," *IEEE Trans. Mobile Comput.*, vol. 13, no. 7, pp. 1443–1455, Jul. 2014.

[16] S. He *et al.*, "Emd: Energy-efficient delay-tolerant p2p message dissemination in wireless sensor and actor networks," *IEEE J. Sel. Areas Commun.*, vol. 31, no. 9, pp. 75–84, Sep. 2013.

[17] C. Huang, R. Zhang, and S. Cui, "Optimal power allocation for outage probability minimization in fading channels with energy harvesting constraints," *IEEE Trans. Wireless Commun.*, vol. 13, no. 2, pp. 1074–1087, Feb. 2014.

[18] A. Liu, J. Ren, X. Li, Z. Chen, and X. Shen, "Design principles and improvement of cost function based energy aware routing algorithms for wireless sensor networks," *Comput. Netw.*, vol. 56, no. 7, pp. 1951–1967, May 2012.

[19] A. Kurs *et al.*, "Wireless power transfer via strongly coupled magnetic resonances," *Science*, vol. 317, no. 5834, pp. 83–86, Jul. 2007.

[20] Powerharvester receivers. [Online]. Available: http://www.powercastco.com

[21] M. Marroncelli, D. Trinchero, V. Lakafosis, and M. M. Tentzeris, "Concealable, low-cost paper-printed antennas for wisp-based RFIDs," in *Proc. IEEE RFID*, 2011, pp. 6–10.

[22] A. K. RamRakhyani, S. Mirabbasi, and M. Chiao, "Design and optimization of resonance-based efficient wireless power delivery systems for biomedical implants," *IEEE Trans. Biomed. Circuits Syst.*, vol. 5, no. 1, pp. 48–63, Feb. 2011.

[23] A. P. Sample, D. J. Yeager, P. S. Powledge, A. V. Mamishev, and J. R. Smith, "Design of an rfid-based battery-free programmable sensing platform," *IEEE Trans. Instrum. Meas.*, vol. 57, no. 11, pp. 2608–2615, Nov. 2008.

[24] Diakinisis automates major distribution center with rfid. [Online]. Available: http://www.lientechnology.com/docs/CS Diakinisis.pdf

[25] T. C. Chen, T. S. Chen, and P. W. Wu, "On data collection using mobile robot in wireless sensor networks," *IEEE Trans. Syst., Man Cybern.*, vol. 41, no. 99, pp. 1–12, Nov. 2011.

[26] M. Lin, H. Rowaihy, T. Bolbrock, G. Cao, and T. La Porta, "Data collection using rfid and a mobile reader," in *Proc. IEEE GLOBECOM*, 2008, pp. 1–6.

[27] O. Tekdas, V. Isler, J. H. Lim, and A. Terzis, "Using mobile robots to harvest data from sensor fields," *IEEE Wireless Commun.*, vol. 16, no. 1, pp. 22–28, Feb. 2009.

[28] Y. Shu, P. Cheng, Y. Gu, J. Chen, and T. He, "Minimizing communication delay in rfid-based wireless rechargeable sensor networks," in *Proc. IEEE SECON*, 2014, pp. 2922–2930.

[29] Motorola mobile rfid reader: Case studies. [Online]. Available: http://www.motorola.com/web/Business/Products/RFID/_Documents/Case_Studies/_StaticFiles/ContinentalAG_Case_Study.pdf

[30] Y. Shi and Y. T. Hou, "Some fundamental results on base station movement problem for wireless sensor networks," *IEEE/ACM Trans. Netw.*, vol. 20, no. 4, pp. 1054–1067, Aug. 2012.

[31] M. Buettner, B. Greenstein, A. Sample, J. R. Smith, and D. Wetherall, "Demo: Rfid sensor networks with the intel wisp," in *Proc. ACM Sensys*, 2008, pp. 1–2.

[32] N. Patwari, A. O. Hero III, M. Perkins, N. S. Correal, and R. J. O'dea, "Relative location estimation in wireless sensor networks," *IEEE Trans. Signal Process.*, vol. 51, no. 8, pp. 2137–2148, Aug. 2003.

[33] N. Malhotra, M. Krasniewski, C. Yang, S. Bagchi, and W. Chappell, "Location estimation in ad hoc networks with directional antennas," in *Proc. IEEE ICDCS*, 2005, pp. 633–642.

[34] K. F. Ssu, C. H. Ou, and H. C. Jiau, "Localization with mobile anchor points in wireless sensor networks," *IEEE Trans. Veh. Technol.*, vol. 54, no. 3, pp. 1187–1197, May 2005.

[35] Y. Shu, P. Cheng, Y. Gu, J. Chen, and T. He. "TOC: Localizing wireless rechargeable sensors with time of charge," *ACM Trans. Sens. Netw.*, vol. 11, no. 3, Jan. 2015, Art. ID. 44.

[36] G. B. Dantzig, *Linear Programming and Extensions*. Princeton, NJ, USA: Princeton Univ. Press, 1998.

[37] E. Welzl, "Smallest enclosing disks (balls and ellipsoids)," *New Results New Trends Comput. Sci.*, vol. 555, no. 1991, pp. 359–370, 1991.

[38] N. Megiddo, "Linear-time algorithms for linear programming in r3 and related problems," in *Proc. IEEE FOCS*, 1983, pp. 329–338.

[39] M. D. Berg, O. Cheong, and M. V. Kreveld, *Computational Geometry: Algorithms and Applications*. New York, NY, USA: Springer-Verlag, 2008.

[40] S. Lloyd, "Least squares quantization in pcm," *IEEE Trans. Inf. Theory*, vol. IT-28, no. 2, pp. 129–137, Mar. 1982.

[41] C. Li, P. Shen, Y. Liu, and Z. Zhang, "Diffusion information theoretic learning for distributed estimation over network," *IEEE Trans. Signal Process.*, vol. 61, no. 16, pp. 4011–4024, Aug. 2013.

[42] P. Shen and C. Li, "Distributed information theoretic clustering," *IEEE Trans. Signal Process.*, vol. 62, no. 13, pp. 3442–3453, Jul. 2014.

[43] T. H. Cormen, *Introduction to Algorithms*. Cambridge, MA, USA: MIT Press, 2001.

[44] K. Vu and R. Zheng, " Geometric algorithms for target localization and tracking under location uncertainties in wireless sensor networks," in *Proc. IEEE INFOCOM*, 2012, pp. 1835–1843.

[45] Y. Zheng and M. Li, "Fast tag searching protocol for large-scale rfid systems," *IEEE/ACM Trans. Netw.*, vol. 21, no. 3, pp. 924–934, Jun. 2013.
[46] N. Alon, D. Moshkovitz, and S. Safra, "Algorithmic construction of sets for k-restrictions," *ACM Trans. Algorithms*, vol. 2, no. 2, pp. 153–177, Apr. 2006.
[47] N. B. Priyantha, H. Balakrishnan, E. D. Demaine, and S. Teller, "Mobileassisted localization in wireless sensor networks," in *Proc. IEEE INFOCOM*, 2005, pp. 1–12.
[48] A. Kurs, R. Moffatt, and M. Soljacic, "Simultaneous mid-range power transfer to multiple devices," *Appl. Phys. Lett.*, vol. 96, no. 4, 2010, Art. ID. 044102.
[49] S. He *et al.*, "Energy provisioning in wireless rechargeable sensor networks," in *Proc. IEEE INFOCOM*, 2011, pp. 2006–2014.
[50] L. Xie, Y. Shi, Y. T. Hou, and H. D. Sherali, "Making sensor networks immortal: An energy-renewal approach with wireless power transfer," *IEEE/ACM Trans. Netw.*, vol. 20, no. 6, pp. 1748–1761, Dec. 2012.
[51] L. He *et al.*, "Esync: An energy synchronized charging protocol for rechargeable wireless sensor networks," in *Proc. ACM Mobihoc*, 2014, pp. 247–256.
[52] Y. Peng, Z. Li, W. Zhang, and D. Qiao, "Prolonging sensor network lifetime through wireless charging," in *Proc. IEEE RTSS*, 2010, pp. 129–139.
[53] B. Tong, Z. Li, G. Wang, and W. Zhang, "How wireless power charging technology affects sensor network deployment and routing," in *Proc. IEEE ICDCS*, 2010, pp. 438–447.

Lingkun Fu (S'14) is currently working toward the Ph.D. degree with the Networked Sensing and Control Group, State Key Laboratory of Industrial Control Technology, Zhejiang University, Hangzhou, China.

His research interests include optimization for wireless rechargeable sensor networks, mobile computing, and cyber–physical systems.

Peng Cheng (M'10) received the B.E. degree in automation and the Ph.D. degree in control science and engineering from Zhejiang University, Hangzhou, China, in 2004 and 2009, respectively.

He is currently an Associate Professor with the Department of Control Science and Engineering, Zhejiang University. His research interests include networked sensing and control, cyber–physical systems, and robust control.

Dr. Cheng served as a Publicity Cochair for the IEEE Tenth IEEE International Conference on Mobile Ad Hoc and Sensor Systems in 2013 and the Local Arrangement Chair for the Association for Computing Machinery International Symposium on Mobile Ad Hoc Networking and Computing in 2015. He serves as an Associate Editor for *Wireless Networks*, the *International Journal of Distributed Sensor Networks*, and the *International Journal of Communication Systems*.

Yu (Jason) Gu (M'10) received the Ph.D. degree from the University of Minnesota Twin Cities, Minneapolis, MN, USA, in 2010.

From 2010 to 2014, he was an Assistant Professor with Singapore University of Technology and Design, Singapore. He is currently a Research Scientist with the Mobile Enterprise Computing Group, Future Systems Department, IBM Research-Austin, Austin, TX, USA. He is the author and coauthor of over 90 papers in premier journals and conferences. His publications have been selected as graduate-level course materials by over 20 universities in the United States and other countries. His research interests include networked embedded systems, wireless sensor networks, cyber–physical systems, wireless networking, real-time and embedded systems, distributed systems, vehicular ad-hoc networks, and stream computing systems.

Dr. Gu is a member of the Association for Computing Machinery.

Jiming Chen (M'08–SM'11) received the B.Sc. and Ph.D. degrees in control science and engineering from Zhejiang University, Hangzhou, China, in 2000 and 2005, respectively.

In 2006, he was a Visiting Researcher with INRIA; in 2007, with the National University of Singapore, Singapore; and from 2008 to 2010, with the University of Waterloo, Waterloo, ON, Canada. He is currently a Full Professor with the Department of Control Science and Engineering and the Coordinator of the Networked Sensing and Control Group, State Key Laboratory of Industrial Control Technology, and the Vice Director of the Institute of Industrial Process Control, Zhejiang University.

Dr. Chen serves/served as the General Symposium Cochair of the Association for Computing Machinery International Wireless Communications and Mobile Computing Conference in 2009 and 2010, as the Medium Access Control Track Cochair for the Fifth International Wireless Internet Conference in 2010, as an Ad Hoc and Sensor Network Symposium Cochair for the IEEE Global Communications Conference and as the Publicity Cochair for the IEEE International Conference on Mobile Ad Hoc and Sensor System (IEEE MASS) and for the IEEE International Conference on Distributed Computing in Sensor Systems in 2011, as the Publicity Cochair for the IEEE International Conference on Distributed Computing Systems (ICDCS) and as the Communications QoS and Reliability Symposium Cochair for the IEEE/CIC International Conference on Communications in China (IEEE ICCC) in 2012, as the Local Chair for IEEE MASS and as the Wireless Networking and Applications Symposium Cochair for IEEE ICCC in 2013, as the Ad Hoc and Sensor Network Symposium Cochair for the IEEE International Conference on Communications in 2014, as the General Vice Chair for the Association for Computing Machinery International Symposium on Mobile Ad Hoc Networking and Computing in 2015, and as The Whole Picture Symposium Cochair for IEEE International Conference on Smart Grid Communications. He was also a Technical Program Committee member for IEEE ICDCS'10,'12,'13, and '14; IEEE MASS'10,'11, and '13; IEEE International Conference on Sensing, Communication, and Networking (SECON)'11 and '12; the IEEE Conference on Computer Communications'11,'12,'13, and '14; *etc.* He currently serves as an Associate Editor for several international journals, including the IEEE TRANSACTIONS ON PARALLEL AND DISTRIBUTED SYSTEMS, the IEEE TRANSACTIONS ON INDUSTRIAL ELECTRONICS, IEEE NETWORK, the IEEE TRANSACTIONS ON CONTROL OF NETWORK SYSTEMS, etc. He was a Guest Editor for the IEEE TRANSACTIONS ON AUTOMATIC CONTROL, *Elsevier Computer Communication*, *Wiley Wireless Communication and Mobile Computer*, and the *Elsevier Journal of Network and Computer Applications*.

Tian He (SM'13) received the Ph.D. degree (under Prof. J. A. Stankovic) from the University of Virginia, Charlottesville, VA, USA, in 2004.

He is currently an Associate Professor with the Department of Computer Science and Engineering, University of Minnesota Twin Cities, Minneapolis, MN, USA. He is the author and coauthor of over 150 papers in premier network journals and conferences with over 14 000 citations (H-Index 48). His research interests include wireless sensor networks, cyber-physical systems, intelligent transportation systems, real-time embedded systems, and distributed systems, and he has been supported by the National Science Foundation, IBM, Microsoft, and other agencies.

Dr. He served in several program/general chair positions and on many program committees at international conferences and currently serves as an editorial board member for six international journals, including the IEEE TRANSACTION ON COMPUTERS and the *ACM Transactions on Sensor Networks*. He has received a number of research awards in the area of networking, including five Best Paper Awards, a National Science Foundation CAREER Award, a K. C. Wong Award, and a McKnight Land-Grant Professorship Award.